Extending Toner Shape Analysis to 3D

Kevin Lofftus, Eastman Kodak Company, Rochester NY/USA

Abstract

Toner shape has been found to influence performance characteristics such as developer flow, transfer, and cleaning. Chemically prepared toner (CPT) manufacturing methods provide control of particle shape, which allows one to optimize the toner performance. Shape analysis using automated digital imaging systems can be used both off-line and on-line to characterize toner shape. Most image analysis methods orient particles to display the two largest dimensions. By combining image analysis with other counting techniques that measure particle volume, such as the Coulter counter method, the minor axis information can be derived and the semi-minor and minor aspect ratios calculated. The inherent errors in edge detection for image analysis must be taken into account.

Introduction

Toner shape influences toner powder flow, bottle fill, developer flow, transfer efficiencies, and cleaning properties in electrophotographic print engines. Control of particle shape is an advantage of chemically prepared toner (CPT) manufacturing methods. Process adjustments affecting size and shape enable the optimization of the toner performance for CPT. Data capture and processing rates for digital cameras have increased to the point where it is now possible to measure and analyze size and shape information real time on a process stream of particles such as CPT. This information can be used for feed back control to adjust size and shape of a CPT using the evaporative limited coalescence (ELC) manufacturing process [1]. Image analysis can only characterize two dimensions of a particle. Orientation effects caused by conditions imposed for high resolution make size correlation with other measurement devices difficult but provide the opportunity to characterize the shape in three dimensions.

Background

For real-time measurements, thin cells are used to take images of a particle stream. The velocity gradient of the laminar flow in the cell will orient the particles so that the major and semi-minor axes are presented to the field of view. The high magnification required for toner-size particles limits the focal plane inside the laminar flow boundary of turbulent flows, making it impossible to eliminate the orientation effects. The resulting size distributions calculated from the images are larger than those measured by other sizing techniques.

Although image analysis is a direct measure of particle properties, its resolution is limited to the wavelength used to image the particle (typically 0.4–0.6 μm). Enlargement and capture can produce images with information at a finer pitch than the image resolution. By integrating over enough light, an intensity gradient can be generated for the edge of a particle at resolutions approaching 0.2 μm.

The computed size of a particle is influenced by the method used to determine the particle edge. Often, a threshold is selected that will exclude the lighter image background. The edge detection may be enhanced by selecting particles in the focal plane that have high intensity gradients at the particle edges. Often, the threshold is selected to just remove the background and thus avoid forming artificial cavities on the low contrast edges of irregular particles.

Spherical particles have high edge contrasts resulting from constructive and destructive interference of light scattered in the near-forward direction. Any reduction in circularity reduces the interferences, and thus irregular particles have lower contrast edges. Also, the intensity gradient extends beyond the particle edge. Mie scattering calculations performed in Matlab by The MathWorks, Inc., based upon FORTRAN code developed by Craig Bohren [2], shows that toner-sized particles remove 2–4 times the light incident on the toner cross section (see Figure 1). This additional light is scattered from outside the particle causing a low intensity gradient that extends well beyond the particle edge. Much of the light is scattered in the forward direction and is captured inside of the particle boundary. This forward-scattered light results in a bight spot in the center of spheres, further defining the edge. However, the forward-scattered light reduces the particle contrast for irregular particles, making edge detection more difficult.

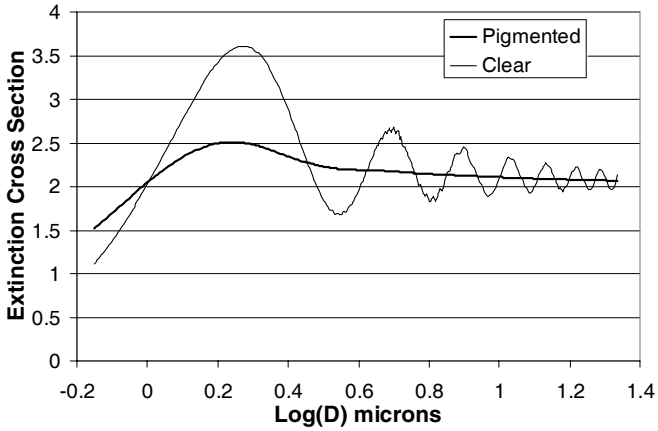

***Figure 1**. Light removed from incident beam relative to that in particle area*

To overcome the limitations of defining edges of irregular particles, a high threshold may be picked and the resulting sizes reduced in some fashion determined by calibration with spheres and a reference measurement. Because image analysis evaluates and counts individual particles, a counting method of high resolution should be used. Photomicrographs taken with SEM using election beams of >5 KV may have high resolution but suffer from highly variable background intensities and edge

gradients, as well as sample preparation difficulties in obtaining uniformly dispersed particles in a dry state. Electric sensing zone (ESZ) devices such as the Coulter counter have a fundamental resolution of volume occupied by single ions but in practice are limited by amplification electronics to 1.5%. A 30 μm aperture may resolve 0.01 μm differences in diameter for a 0.7 μm particle, and 0.1 μm differences for toner-sized particles.

Once the particle edge is defined, the area of the particle may be determined and shape characterization performed. Common shape characterizations are circularity and aspect ratio. Aspect ratios are usually reported as the ratio of the major axis length over the minor axis. Circularity is the ratio of perimeter to that of a circle having an equal area. The standard definition of these metrics leads to ranges from 1 to infinity. It is convenient to use the inverse ratios so that the data are bounded by 0 and 1. An inverse aspect ratio $R_{min\text{-}max}$ can be defined as the maximum distance across the particle perpendicular to the major axis divided by the maximum length parallel to the major axis. The major axis direction is usually defined as perpendicular to parallel lines oriented to obtain the greatest separation while touching the edge.

Materials and Methods

A shape series of 8 μm CPT were made using a polyester binder, copper phthalocyanine pigment at a level to give a covering power of ~2000 cm^2/g, and various levels of shape control additive (SCA) (see Table 1) to obtain approximately equal changes in the inverse aspect ratio $R_{min\text{-}max}$. These toners were compared to a melt pulverized toner (MPT) made with similar materials. Dispersions of these toners were made using a combination of an ionic and two nonionic surfactants. The dispersions were measured using a Coulter counter IIE with an internally purged 30 μm aperture [3, 4] and imaged with an FPIA-3000 (manufactured by Sysmex Corporation and distributed by Malvern Instruments) using a 10X objective and a threshold of 85% of the average background intensity. SEM microphotographs were taken for comparison on a LEO 1415VP (made by Carl Zeiss SMT Inc.). The particles were gold coated and measured at 5KV at 1000X magnification.

The Sysmex calibration and focusing were performed using 2 μm clear spherical polystyrene beads from Duke. The size calibration was verified with Coulter counter measurements using these beads as well as seven spherical clear beads ranging in size from 3 to 17 μm made from polyester using the ELC process, and three spherical clear beads ranging in size from 30 to 80 μm made from vinyl toluene or styrene divinyl benzene copolymers using polymerization-limited coalescence. Good agreement with Coulter measurements was found for the circularly equivalent diameters (*Dce*) reported by Sysmex but not when computed from the reported Sysmex area (*S*) using the formula

$$D_{ce} = 2\sqrt{S/\pi}\,. \qquad (1)$$

The error in diameters was significant and found to be 0.6 μm when the mode of the distributions was matched for particle sizes up to ~10 μm. The error in diameter increased for increasing particle sizes >10 μm (see Figure 2).

Colored spherical beads made by ELC were used to test the effect of forward light scattering on edge detection. The cyan and magenta toners were ~5.5 μm and increase the error to ~0.75 μm. A black 5.5 μm toner gave an error of 0.9 μm while a 4 μm yellow toner was similar to clear toners. These differences are consistent with the detection wavelengths of a charge-coupled device (CCD) used in the digital camera.

Table 1: Shape Series of Toners

Type	SCA	Intr	Images
CPT	0	SEM	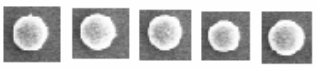
		FPIA	
	1	SEM	
		FPIA	
	2	SEM	
		FPIA	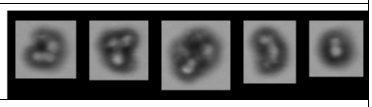
	3	SEM	
		FPIA	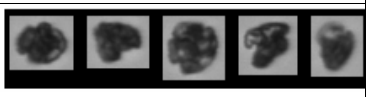
MPT	NA	SEM	
		FPIA	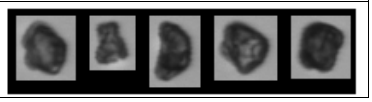

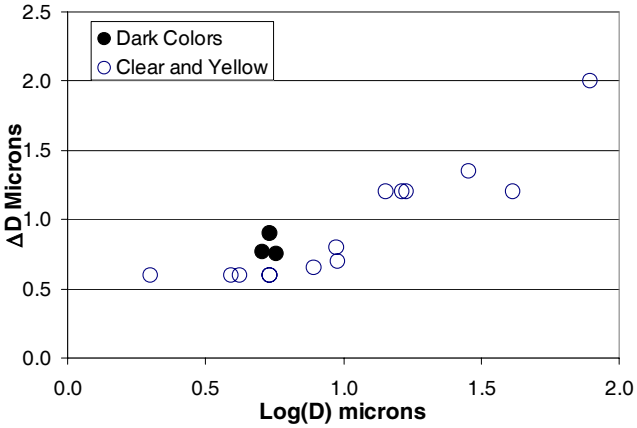

***Figure 2**. Difference in Sysmex and Coulter D_{ce} vs. bead size*

The Sysmex FPIA-3000 allows one to produce a text file containing the XY pair locations of each of the edge pixels for each valid particle. A routine using the visual basic add-in in Microsoft Excel was developed to read and process these text files. Cells in the Excel worksheet were filled to match the image with different characters to aid in new algorithm development. The resulting information was then compared to the Coulter size distribution in Excel to develop a three-dimensional shape analysis.

Results

Data Fitting Methods

New algorithms were developed for cavity exclusion, center location, major axis angle detection, perimeter fitting, and aspect ratio. The area was computed using the internal pixels plus one-half of the perimeter pixels to be consistent with locating and fitting algorithms that effectively use the center of the perimeter pixels. The Sysmex software uses all of the edge pixels in computing the area. Using only one-half of the edge pixels for the particle area reduces the error in *Dce* (compared to Coulter) by ~0.31 μm.

The focus and calibration had shifted slightly from the data acquired to generate Figure 2, so the spherical CPT from the shape series was used to verify the Sysmex calibration. The edge shift and pixel calibration were picked by matching the mode width and minimizing the sum squared error between the Sysmex and Coulter size distributions. The three-dimensional shape analysis is more sensitive to adjusting the calibration because the influence of area reduction and diameter shift on the aspect ratio could be taken into account when estimating the calibration.

An ellipse was chosen as a model shape for image analysis because its three-dimensional analog, the ellipsoid, is easy to understand and use. New algorithms were required to fit an ellipse to the perimeter. The center location was computed as the average of the edge pixel location distance to the initial center estimate, excluding those for cavities deeper than 0.7 times that of the perpendicular distance from a line across the cavity mouth to the initial estimate of the center location . An average radius R_0 was computed and the angles to the ends of the perimeters at the cavities (α_{ccw} and α_{cw}) were calculated. If one cavity was excluded, the center location was adjusted. The Sysmex perimeter file output proceeds in a counterclockwise fashion, so the adjustment in center location is:

$$\begin{aligned} X_{C1} &= X_{C0} + R_0\left(Sin\left(\alpha_{ccw}\right) - Sin\left(\alpha_{cw}\right)\right) \\ Y_{C1} &= Y_{C0} - R_0\left(Cos\left(\alpha_{ccw}\right) - Cos\left(\alpha_{cw}\right)\right) \end{aligned} \quad (2)$$

The direction of the major axis (β) was located by finding the angles of opposing maxima to the new center (after some averaging to remove pixelization effects). Often, two maxima were near each other and the average weighted by the distance to center was used to compute an angle from center to be used as one of the opposing maxima angles. β was calculated as the angle of the greatest maximum adjusted by one-half of the difference of the opposing angle plus π.

An ellipse with the major axis direction of β centered at (X_{C1},Y_{C1}) was then fit using a numerical method to minimize the simultaneous sum-squared error from the $\sin^2(\beta)$ and $\cos^2(\beta)$ weighted distance squared from the edge to the center. By retaining the signed of the averaged error squared, the step direction and amount could be estimated for changes in the major (a) and semi-minor (b) axes. The initial values for the numerical methods was found by solving for the linear equation set for the least-squared error in terms of the weighted reciprocal squared axes (a^{-2}, b^{-2}).

The spherical equivalent diameter D_{se}, measured by the Coulter counter, was equated to the major axis a and to the semi-minor and minor inverse aspect ratios R_b (= b/a) and R_c (= c/a) by equating the volume of a sphere to an ellipsoid having a minor axis:

$$V = \pi D_{se}^3/6 = \pi a R_b R_c/6 \quad \therefore D_{se} = a\left(R_b R_c\right)^{1/3}. \quad (3)$$

The expression D_{se} is substituted into the area equation for an ellipse:

$$A = \pi a^2 R_b/4\left(R_b R_c\right)^{1/3} = \pi {D_{se}}^2 R_b^{2/3}/4\,R_c^{1/3}. \quad (4)$$

The average R_b from the least square fit with ellipses and D_{se} from the Coulter channels are used to bin the Sysmex areas into a size distribution with R_c adjusted to minimize the sum-squared error between the Sysmex and Coulter distributions.

Discussion

A very good fit of Sysmex data to Coulter data was obtained for samples with good dispersions and low enough concentrations to avoid coincidence in either instrument (see Figure 3). The fit to the area calculated from the least-squared error ellipses was not significantly different except for a reduction in pixelization noise. The equivalency of the fits was true because the area of the fit ellipses were not significantly different from the imaged area.

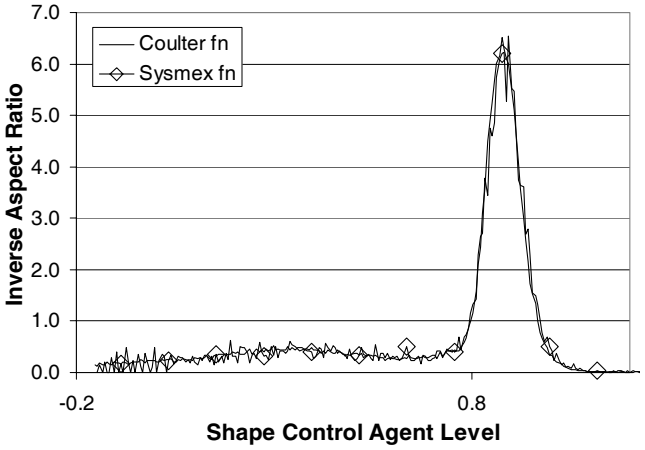

***Figure 3**. Fit of Sysmex to Coulter PSD for CPT sample with SCA level 3*

The data for the non-spherical CPT and MPT samples were fit using the values determined from the spherical SPT by varying only the minor axis inverse aspect ratio R_c. Applying the edge shift to the major and semi-minor axes before computing $R_{min\text{-}max}$ resulted in values very similar to the R_b-computed values from the fit ellipses.

Comparing the semi-minor and minor inverse aspect ratios R_b and R_c showed a steady decease in R_b but a sudden drop in R_c between the SCA levels 1 and 2 (see Figure 4). This transition

occurred where folds appeared in the SEM photomicrographs (see Table 1). Few folds appeared on the edges and were not imaged in the Sysmex as cavities at the threshold used. The volume of the folds is not measured by Coulter and was represented by a decrease in minor axis dimension. Note that R_c was less than R_b when there were no folds for CPT samples, as expected for orientation in laminar flows.

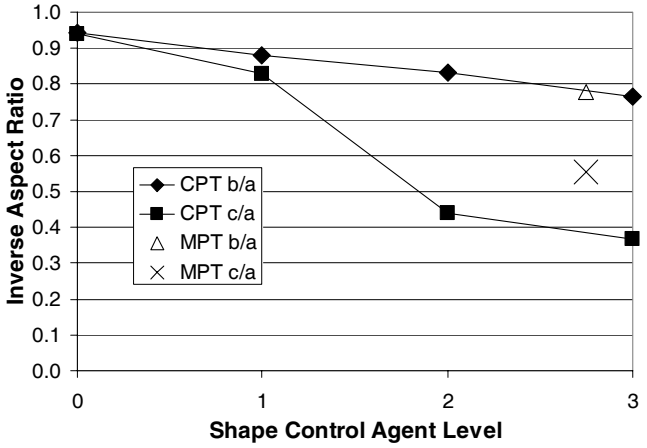

***Figure 4**. Inverse aspect ratios for CPT vs. SCA and MPT at arbitrary point*

A third characterization method may be used to determine the amount of volume in the folds. For example, a method using the ratio BET-to-ellipsoid surface areas could be developed. Another possibility is the analysis of the number and size distribution of forward-scattered light responsible for the lighter spots within a particle perimeter. A third possibility is to use a measurement technique that includes the volume of the folds such as sizing by sedimentation

The lower contrast for CPT samples with folds suggests that there may have been a change in edge detection resulting from the loss of interference of scattered light. There were no folds and only shallow cavities for the MPT, but R_c was significantly lower than R_b. An additional edge shift of 0.6 μm would be required to move R_c from 0.55 to 0.72. SEM photomicrographs show highly shaped particles of MPT for the particular grinding process and polyester used to make this sample. Any change in edge shift because of changes in light scattering for rough or folded toner particles is likely to be limited to <0.2 μm.

The difference in R_c between CPT and MPT at the same R_b was very significant and was due to the deep folds that formed for these CPT samples. This difference would lead to lower packing densities and bottle fill. Other performance characteristics resulting from these folds are more difficult to predict, and require testing to determine. The direction of the performance shift would be to greater R_c, lower density, higher surface area, and lower contact.

Conclusion

Image analysis shape and size distributions can be used in combination with Coulter counter size distributions to characterize 3D shape. Light-scattering effects on the edge detection must be taken into account when developing methods to calibrate the images sizes. Calibration at a constant threshold using spherical toners showed a shift in the location edge and resulted in an increase in diameter 0.6 μm for clear, 0.75 μm for cyan and magenta toner, and 0.9 μm for black toner.

An average semi-minor axis aspect ratio can be calculated from the least-squared error fit of ellipses to the perimeters of the toner images. This information can be combined with the Coulter size distribution to estimate the average minor axis aspect ratio.

Folds are formed in CPT when using ELC with SCA and the semi-minor aspect ratio approaches that of MPT. The volume of the folds is not measured by the Coulter counter. Most of the fold area is not seen at the perimeter of CPT in images and therefore is not excluded. Including the fold volume resulted in very low estimates for the minor axis inverse aspect ratio.

The combination of image analysis and Coulter counter sizing provides a good method of three-dimensional shape characterization. This method may be combined with other techniques to further characterize toner particles. This information can be correlated with performance changes for toner.

References

[1] M. Nair, Z. Pierce, and C. Sreekumar, US Patent 4833060, 1989.

[2] C. F. Bohren and D. R. Huffman, Absorption and Scattering of Light by Small Particles (Willey, New York, NY, 1983) pg. 479.

[3] K Lofftus, Improvements in Toner Fines Characterization, Proc. NIP21 (IS&T, Baltimore, MA, 2005) pp. 484–487.

[4] K Lofftus, Time Discrimination of Coulter Recount Artifact, Proc. NIP22 (IS&T, Denver, CO, 2006) pp. 161–164.

Author Biography

Kevin Lofftus received a B. S. in 1982 and a M. S. in 1984 for Mineral Process Engineering from Montana College of Mineral Science and Technology and a Ph. D. in 1989 from The University of California Berkeley for Mineral Processing with minors in Chemical Engineering and Statistics. He joined the Copy Products Division of Kodak in 1989 and is currently a Research Scientist at Eastman Kodak Company.